

Quantum phases of bosons in double-well optical lattices

I. Danshita^{1,2}, J. E. Williams³, C. A. R. Sá de Melo^{1,4}, and C. W. Clark¹

¹*Joint Quantum Institute, National Institute of Standards and Technology, and University of Maryland, Gaithersburg, Maryland 20899, USA*

²*Department of Physics, Waseda University, 3-4-1 Ōkubo, Shinjuku, Tokyo 169-8555, Japan*

³*Wolfram Research, Inc., Champaign, IL 61820, USA*

⁴*School of Physics, Georgia Institute of Technology, Atlanta, Georgia 30332, USA*

(Dated: November 4, 2018)

We study the superfluid to Mott insulator transition of bosons in a two-legged ladder optical lattice, of a type accessible in current experiments on double-well optical lattices. The zero-temperature phase diagram is mapped out, with a focus on its dependence upon interchain hopping and the tilt between double wells. We find that the unit-filling Mott phase exhibits a non-monotonic behavior as a function of the tilt parameter, producing a reentrant phase transition between Mott insulator and superfluid phases.

PACS numbers: 03.75.Hh, 03.75.Lm, 05.30.Jp, 73.43.Nq

Optical lattices loaded with ultra-cold atoms provide the opportunity to study quantum phases of many-particle systems because of their unprecedented degree of controllability [1]. Presently the lattice depth, dimensionality, geometry, and filling factor can all be reasonably controlled. While one of the first examples of this degree of control was the experimental observation of the superfluid (SF)-to-Mott insulator (MI) transition in three-dimensional cubic optical lattices as a function of the lattice depth [2], tetragonal and orthorhombic optical lattices can also be produced by deepening the optical potential along desired directions [3, 4].

More recently, possibilities for control have expanded with the experimental realization of double-well optical lattices. Control of the polarization of the laser beams allows for the production of lattices with a base in two and three dimensions [5] as illustrated in Fig. 1a, where Bose atoms (⁸⁷Rb) have been successfully trapped. In particular, one can create a one-dimensional double-well optical lattice corresponding to a two-leg ladder structure shown in Fig. 1b by increasing the long period of the double-well optical lattice. In standard condensed-matter physics, a few compounds, such as vanadyl pyrophosphate (VO)₂P₂O₇ [6] and some cuprates like SrCu₂O₃ [7], have such two-leg ladders in their crystalline structure, and they display much of the interesting physics encountered in general ladder systems, associated with the interplay between spin-gapped and superconducting states [8]. However, conventional condensed-matter systems come with fixed dynamical and structural parameters, while the flexible variability of optical lattices offers the prospect of exploring the full parameter space. Moreover, the particles confined in the current double-well optical lattices are bosonic atoms, in contrast to conventional condensed-matter systems, where electrons (fermions) dictate the quantum phases.

In this paper, we study the zero-temperature phase diagram of bosons in double-well optical lattices. We focus on the case of a two-legged ladder, where analytical and numerical progress can be made; in particular, we ap-

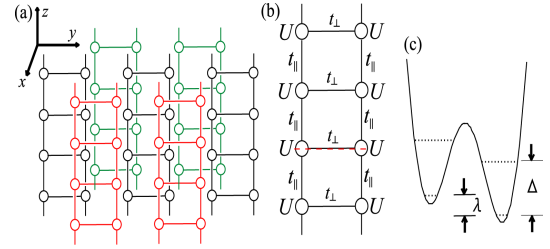


FIG. 1: (a) Schematic picture of a 3D configuration of a double-well lattice. Circles represent sites, and solid lines represent connections via the hopping between sites. (b) Schematic picture of the two-leg ladder. (c) Double-well potential corresponding to the cross section for the dashed line in (a). Dotted lines represent the energy levels for each well.

ply the time-evolving block decimation (TEBD) [12, 13] method to such ladder systems. We show that the phase diagram changes dramatically as a function of the chemical potential μ , the intrachain (interchain) hopping t_{\parallel} (t_{\perp}), the on-site repulsion U and the tilt λ of the double-well, which are indicated in Figs. 1b and 1c. For $\lambda = 0$ and different ratios t_{\perp}/U , Mott phases with half-integer (in addition to integer) filling factors emerge in the phase diagram of μ/U versus t_{\parallel}/U for small ratios of t_{\perp}/U . As t_{\perp}/U increases, the half-filling MI phase becomes larger and the unit-filling one becomes smaller. For fixed ratio t_{\perp}/U , and different values of λ/U , we also obtain the μ/U versus t_{\parallel}/U phase diagram which reveals a reentrant phase transition for the unit-filling MI induced by the tilt λ . The reentrant phase transition can be attributed to the development of coherence in each double well in the vicinity of $\lambda = U$ which drives the system into the SF phase. Finally, we also calculate the critical points for the MI-to-SF transition at half and unit fillings.

To describe the physics discussed above, we introduce the Bose-Hubbard model for the double-well ladder

$$H = \sum_i [H_i^{\text{dw}} - t_{\parallel} \sum_{\eta \in \{L,R\}} (a_{i+1,\eta}^{\dagger} a_{i,\eta} + \text{h.c.})], \quad (1)$$

where H_i^{dw} represents the double-well Hamiltonian for a given ladder index i and is given by

$$H_i^{\text{dw}} = \sum_{\eta} \left[\frac{U}{2} \hat{n}_{i,\eta} (\hat{n}_{i,\eta} - 1) - \mu \hat{n}_{i,\eta} \right] - t_{\perp} (a_{i,R}^{\dagger} a_{i,L} + \text{h.c.}) + \frac{\lambda}{2} (\hat{n}_{i,L} - \hat{n}_{i,R}), \quad (2)$$

$a_{i,\eta}^{\dagger}$ creates a boson at the lowest level localized on the left (right) of the i -th double-well when $\eta = L$ (R). We do not include the effect of the harmonic trapping potential. We assume that all the parameters are sufficiently small compared to the energy gap Δ between the first and second levels of each site. Furthermore, all parameters of H are controllable in experiments [5], and thus we begin our discussion by analyzing the limit of $t_{\parallel} = 0$.

Integer and Half-Integer Mott Phases: When $t_{\parallel} = 0$ several MI phases emerge. In this case, the Hamiltonian Eq. (1) reduces to $H = \sum_i H_i^{\text{dw}}$. One can obtain the eigenenergy $E^{(0)}(n, j)$ and eigenstate $|\Phi_{n,j}\rangle = \sum_{n_L=0}^n C_{n_L}(n, j) |n_L, n-n_L\rangle$ of H_i^{dw} , where n is the number of atoms in each double well and the quantum number j is a non-negative integer less than $n+1$ ($j = 0, 1, \dots, n$). $|n_L, n_R\rangle$ is the Fock state with n_L (n_R) atoms on the left (right) of each double well. When n is even (odd), the filling factor ν of the MI phases is integer (half-integer). Although there exists a MI phase for each value of n , we focus here only on the $\nu = 1, 1/2$ phases.

We consider first the case of symmetric double wells ($\lambda = 0$) and discuss two limiting situations corresponding to $t_{\perp} \gg U$ and $t_{\perp} \ll U$. For $t_{\perp} \gg U$, the anti-bonding single particle state of the double-well is pushed to energies much higher than U , and only the bonding single particle state and the lowest energy two-particle state are important. Therefore, in this limit, the $\nu = 1/2$ ($\nu = 1$) phase can be mapped into the unit (double)-filling MI phase for a 1D lattice with an effective hopping t_{\parallel} and an on-site repulsive interaction $U/2$. For $t_{\perp} \ll U$, the $\nu = 1$ MI phase approaches that of a 1D lattice (two independent filling-one chains), and the width of the $\nu = 1$ MI phase on the μ -line is $\sim U$. In the strict limit of $t_{\perp} = 0$, the $\nu = 1/2$ MI phase vanishes and the system is always a superfluid since there is a low energy path for the bosons to move along the chains.

Next, we consider the case of tilted double wells, where $\lambda \neq 0$. The MI states present in the double-well ladders discussed here are quite different from those encountered in strictly 1D superlattices [9]. When $\lambda \gg \max(t_{\perp}, U)$, the MI with filling ν in the double-well ladder reduces to the MI with 2ν in a single 1D lattice. In this regime, a transition to a SF phase occurs at a critical t_{\parallel} in contrast to the case of the 1D superlattice, where all the occupied wells are completely isolated from each other and the system remains always in the MI phase.

We discuss two special cases $\lambda = U$ with $t_{\perp} \ll U$ and $\lambda \gg \max(t_{\perp}, U)$. For $\lambda = U$ and $t_{\perp} \ll U$, where the states $|1, 1\rangle$ and $|0, 2\rangle$ are nearly degenerate, the width of the $\nu = 1$ MI phase on the μ -line is reduced to $\sim 2\sqrt{2}t_{\perp}$.

However, for $\lambda \gg \max(t_{\perp}, U)$, the width of the $\nu = 1$ MI phase is $\sim U$. This happens because the $\nu = 1/2, 1$ MI phases in a double-well ladder reduce to the unit- and double-filling MI phases of a single 1D lattice, as all bosons prefer to be in the lowest energy side of the largely tilted double well.

These special cases reflect the more general trend that as λ increases, width of the $\nu = 1$ MI phase on the μ -line changes non-monotonically. Such non-monotonic behavior for the $\nu = 1$ MI phase is also found in (μ, t_{\parallel}) -plane for varying values of λ and will be discussed next by taking into account finite t_{\parallel} and studying the insulator to superfluid transition.

Insulator to Superfluid Transition-I: To include the effects of t_{\parallel} and study the MI-to-SF transition, we use first a perturbative mean-field approach (PMFA) [10]. Although PMFA fails to describe 1D systems quantitatively [11], it provides qualitative understanding and analytical insight. Quantitative results can be obtained using the TEBD method [12, 13]; these results are compared later with the picture that emerges from PMFA.

We consider the effects of finite t_{\parallel} and introduce the SF order parameter $\psi_{\eta} = \langle a_{i,\eta} \rangle = \langle a_{i,\eta}^{\dagger} \rangle$ into the Hamiltonian Eq. (1), which reduces to

$$H \simeq \sum_i H_i^{\text{mf}} = \sum_i [H_i^{\text{dw}} + 2t_{\parallel} \sum_{\eta} \psi_{\eta}^2 + V_i], \quad (3)$$

where $V_i = -2t_{\parallel} \sum_{\eta} \psi_{\eta} (a_i^{\dagger} + a_i)$ describes the transfer of atoms between i -th sites and the condensate ψ_{η} and is treated perturbatively.

Using perturbation theory, we obtain the correction $\Delta E_n = E_n - E^{(0)}(n, 0)$ to the unperturbed ground state energy $E^{(0)}(n, 0)$ in terms of ψ_{η} . Performing a linear transformation $(\Psi_1, \Psi_2)^{\dagger} = X(\psi_L, \psi_R)^{\dagger}$ to diagonalize the quadratic part of ΔE_n leads to

$$\Delta E_n = \sum_{\zeta \in \{1,2\}} A_{\zeta}(n, \bar{t}_{\perp}, \bar{t}_{\parallel}, \bar{\mu}) \Psi_{\zeta}^2 + O(\Psi_1^4, \Psi_1^3 \Psi_2, \dots), \quad (4)$$

where X is a 2 by 2 Hermitian matrix and the bars on parameters mean the normalization by U , e.g. $\bar{\mu} \equiv \mu/U$. Expressions for the coefficients of Ψ_{ζ}^2 and fourth order terms are quite long, thus we will not give them here. However, A_2 is always positive, while A_1 changes sign, and the fourth order coefficients are positive, leading to second-order phase transitions between the MI ($\Psi_1 = \Psi_2 = 0$) and SF ($\Psi_1 \neq 0, \Psi_2 = 0$) states.

For symmetric double wells ($\lambda = 0$), we obtain analytical expressions for the MI-SF phase boundary ($A_1 = 0$) in two limits. When $t_{\perp} \ll U$, the phase boundaries are

$$\bar{t}_{\parallel}^{\text{pb}} \simeq \begin{cases} \frac{\bar{t}_{\perp}^2 - \bar{\mu}^2}{4\bar{t}_{\perp}}, & n = 1 \quad (\nu = 1/2), \\ \frac{(\bar{\mu} - \bar{t}_{\perp})(-\bar{\mu} + 1 - 2\bar{t}_{\perp})}{2(\bar{\mu} + 1)}, & n = 2 \quad (\nu = 1), \end{cases} \quad (5)$$

In this case, the critical value of t_{\parallel} is

$$t_{\parallel}^{\text{c}} \simeq \begin{cases} \frac{1}{4} t_{\perp}, & n = 1 \quad (\nu = 1/2), \\ \frac{3-2\sqrt{2}}{2} U - \frac{1}{2} t_{\perp}, & n = 2 \quad (\nu = 1), \end{cases} \quad (6)$$

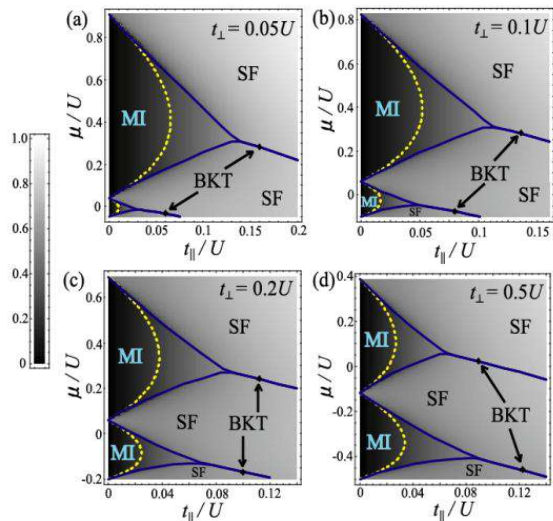


FIG. 2: Phase diagrams for symmetric double wells. Dashed lines represent the phase boundary calculated within PMFA. Solid lines, density plots, and dots are calculated by the infinite-TEBD. \tilde{n} is integer inside the solid lines. The density plots represent σ . The dots represent the critical point of the BKT transition.

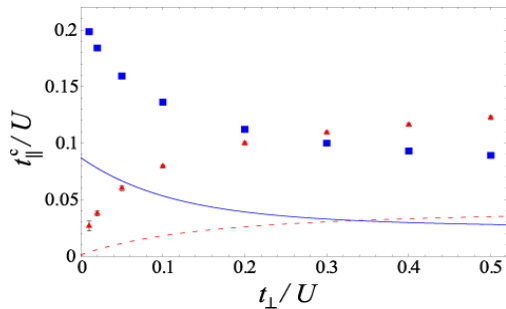


FIG. 3: Critical intra-chain hopping t_{\parallel}^c for symmetric double wells as a function of t_{\perp} . Dashed and solid lines represent t_{\parallel}^c 's for the half- and unit-filling MI phases calculated within PMFA. Triangles and squares represent t_{\parallel}^c 's for the half- and unit-filling MI phases calculated by the infinite-TEBD.

with $\mu_c \simeq 0$ for $\nu = 1/2$ and $\mu_c \simeq (\sqrt{2} - 1)U$ for $\nu = 1$. In the case of $t_{\perp} \gg U$, the double-well system reduces effectively to a single 1D lattice, and the phase boundaries as well as the value t_{\parallel}^c can be obtained from the standard results [10] by replacing $U \rightarrow U/2$.

In Fig. 2, the MI-SF phase boundaries for $\lambda = 0$ calculated within PMFA are shown as dashed lines for different values of t_{\perp} . Notice that the figures are not in the same scale. In Fig. 3, the critical intra-chain hoppings t_{\parallel}^c 's for the $\nu = 1/2, 1$ MI phases are shown as functions of t_{\perp} as dashed and solid lines. The $\nu = 1/2$ ($\nu = 1$) MI lobe grows (shrinks) since t_{\parallel}^c increases (decreases) with increasing t_{\perp} so that the double-well system reduces to a single 1D system in the limit of $t_{\perp} \gg U$.

Next, we discuss the case of tilted double wells ($\lambda \neq 0$).

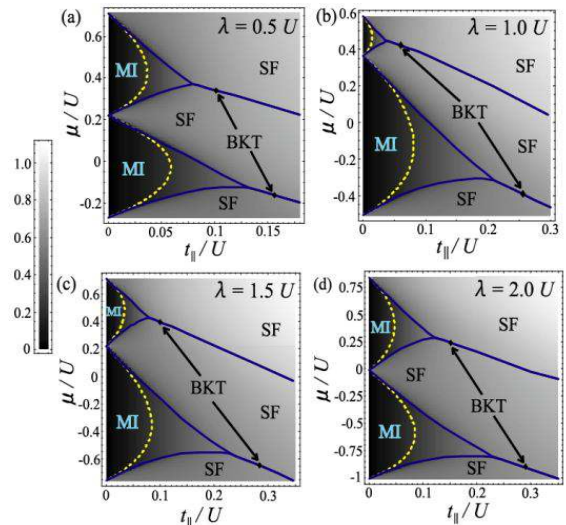


FIG. 4: Phase diagrams for tilted double wells ($t_{\perp} = 0.1U$).

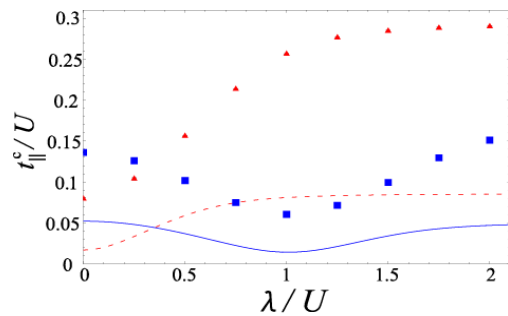


FIG. 5: t_{\parallel}^c 's for $t_{\perp} = 0.1U$ as a function of λ (Error bars are smaller than the size of symbols).

In Fig. 4, we show the MI-SF phase boundaries for different values of λ at fixed $t_{\perp} = 0.1U$ indicated by dashed lines. In Fig. 5, we show the critical intra-chain hoppings t_{\parallel}^c 's versus λ for the $\nu = 1/2, 1$ MI phases indicated by dashed and solid lines, respectively. The $\nu = 1/2$ MI lobe or t_{\parallel}^c grows monotonically as λ increases. In contrast, the $\nu = 1$ MI lobe or t_{\parallel}^c changes non-monotonically as a function of λ .

This non-monotonic behavior for $\nu = 1$ can be understood as follows: at $\lambda = 0$, t_{\parallel}^c is given approximately by Eq. (6) since $t_{\perp} \ll U$ when $t_{\perp} = 0.1U$. As λ increases, t_{\parallel}^c initially decreases. At $\lambda = U$, t_{\parallel} reaches a minimum when $t_{\parallel}^c \simeq \sqrt{2}t_{\perp}/6$, since the states $|1, 1\rangle$ and $|0, 2\rangle$ states are nearly degenerate, i.e., the local state of the MI phase at $\lambda = U$ is $|\Phi_{2,0}\rangle \simeq (|1, 1\rangle + |0, 2\rangle)/\sqrt{2}$. The development of this local coherence then pushes the system into the SF phase. Further increase of λ moves the system away from this degeneracy which favors SF, and forces t_{\parallel}^c to increase causing a reentrance into a MI phase. In particular, when $\lambda \gg U$ all atoms move to a single chain and are in $|0, 2\rangle$, thus the critical value becomes $t_{\parallel}^c \simeq (5 - 2\sqrt{6})U/2$ as

expected for a single chain [10].

The non-monotonic behavior of t_{\parallel}^c shows a reentrant quantum phase transition from MI to SF to MI, induced by the tilt λ when t_{\parallel}^c is kept between $(t_{\parallel}^c)_{\min}$ and $(t_{\parallel}^c)_{\max}$. Taking into account the high degree of control achieved in double-well optical lattices [5], we expect this reentrance to be observed experimentally. However, since we do not expect PMFA to give quantitatively correct results for the double-well (ladder) optical lattice, we next discuss numerical results using the TEBD method.

Insulator to Superfluid Transition-II: To determine quantitatively the phase diagrams for double-well (ladder) optical lattices, we use the infinite-size version of TEBD [13], which provides an excellent ground state for 1D quantum lattice systems via imaginary time evolution. To apply the TEBD method to our problem, we map the double-well (ladder) Bose-Hubbard model into a single chain with *next-nearest-neighbor* hopping, whose ground state can be calculated via the *swapping* technique [14]. We note that the infinite-TEBD algorithm has been recently applied to single chains with *only nearest-neighbor* hopping, where the quantum Berezinskii-Kosterlitz-Thouless (BKT) critical point [15] was obtained for the unit-filling case. While the maximum number of bosons per site is $N_{\max} = \infty$, convergence is already achieved in our numerical calculations, when $N_{\max} = 4$ for $\nu = 1/2$ and $N_{\max} = 5$ for $\nu = 1$.

The phase diagrams in the (μ, t_{\parallel}) -plane are shown in Figs. 2 and 4, where the solid lines indicate the MI-SF phase boundaries, which have roughly a triangular shape. The sides of the MI lobe, the phase transition occurs from a $\nu = 1/2, 1$ MI to a SF with $\nu \neq 1/2, 1$. However, the two sides of the “triangle” merge for each MI phase (see dots in Figs. 2 and 4) producing a phase transition from a $\nu = 1/2, 1$ MI to a SF with $\nu = 1/2, 1$, which is of the BKT type [11, 16].

To locate the phase boundaries we calculate directly the mean number of atoms per double well $\tilde{n} \equiv \sum_{\eta} \langle \hat{n}_{i,\eta} \rangle$, but we also calculate the fluctuation $\sigma \equiv \sqrt{\langle \hat{n}_i^2 \rangle - \langle \hat{n}_i \rangle^2}$, which is small deep in the MI regions, and relatively large in the SF regions. Since we are interested in local observables, such as \tilde{n} and σ , convergence is already achieved for $\chi = 15$, where χ is the size of the basis set retained in the TEBD procedure [12].

We locate the BKT transition on the lines of integer \tilde{n} ($\nu = 1/2, 1$) by calculating the correlation function $\langle \hat{\alpha}_i^{\dagger} \hat{\alpha}_0 \rangle$, where $\hat{\alpha}_i^{\dagger}$ creates an atom in the lowest single par-

ticle state of a double-well. The SF phase of the double-well ladder can be regarded as a two-band Tomonaga-Luttinger liquid (TLL), and the correlation function exhibits power-law decay as $\langle \hat{\alpha}_r^{\dagger} \hat{\alpha}_0 \rangle \propto r^{-K/2}$. The exponents K_c at the phase transitions can be calculated from the TLL theory. For instance, when $\max(t_{\perp}, \lambda) \gg U$, our system is effectively a single 1D chain and has the critical value $K_c = 1/2$ for the BKT transition [11]. In addition, when $\lambda = 0$ and $\tilde{n} = 2$ ($\nu = 1$), the critical value is also $K_c = 1/2$ [16]. Consequently we use the criterion $K_c = 1/2$ to identify the critical point for the BKT transition at integer values \tilde{n} ($\nu = 1/2, 1$).

We calculate K as a function of t_{\parallel} by fitting $a \cdot r^{-K/2}$ to the correlation function calculated from the TEBD method with $\chi = 60$. We use the intervals $10 \leq r \leq 15$, $15 \leq r \leq 20$, $20 \leq r \leq 25$, and $25 \leq r \leq 30$ for the fit and take the average of them to produce error bars. The critical intra-chain hopping t_{\parallel}^c along the lines of integer \tilde{n} is determined when $K = K_c$. The dots in Figs. 2 and 4 correspond to the BKT transition points. In Figs. 3 and 5, t_{\parallel}^c 's for $\tilde{n} = 1, 2$ ($\nu = 1/2, 1$) are shown as triangles and squares, respectively. The phase boundaries asymptotically approach those of PMFA as t_{\parallel} tends to zero. On the other hand, differences between PMFA and TEBD are significant when t_{\parallel} is relatively large. In particular, t_{\parallel}^c obtained using TEBD is more than twice as large as that obtained within PMFA. However, the qualitative behavior of the phase diagram as a function of t_{\perp} and λ obtained within PMFA is consistent with that of the infinite-TEBD.

Conclusions: In summary, we have studied the superfluid-to-Mott insulator transition of bosons in double-well (ladder) optical lattices. Applying the time-evolving block decimation (TEBD) method to the two-leg Bose-Hubbard model, we have calculated the zero-temperature phase diagram. We have found that the phase diagram changes significantly depending on the inter-chain hopping and tilt of the double wells. In particular, we have shown that the tilt can be used to induce reentrant transitions between Mott insulator and superfluid phases. Through a comparison of the results of TEBD and the perturbative mean-field approach (PMFA), we have shown that PMFA fails to describe the phase diagram quantitatively, but captures its qualitative trends.

We acknowledge support from a Grant-in-Aid from JSPS (I. D.) and from NSF-DMR-0304380 (C. SdM.).

[1] D. Jaksch *et al.*, Ann. Phys. (N.Y.) **315**, 52 (2005).

[2] M. Greiner *et al.*, Nature **415**, 39 (2002).

[3] I. B. Spielman *et al.*, Phys. Rev. Lett. **98** 080404 (2007).

[4] T. Stöferle *et al.*, Phys. Rev. Lett. **92**, 130403 (2004).

[5] J. Sebby-Strabley *et al.*, Phys. Rev. A, **73**, 033605 (2006).

[6] D. C. Johnston *et al.*, Phys. Rev. B **35**, 219 (1987).

[7] M. Azuma *et al.*, Phys. Rev. Lett. **73**, 3463 (1994).

[8] E. Dagotto, Rep. Prog. Phys. **62**, 1525 (1999).

[9] P. Buonsante *et al.*, Phys. Rev. A **70**, 033608 (2004).

[10] D. van Oosten *et al.*, Phys. Rev. A **63**, 053601 (2001).

[11] T. D. Kühner *et al.*, Phys. Rev. B **61**, 12474 (2000).

[12] G. Vidal, Phys. Rev. Lett. **91**, 147902 (2003); *ibid.* **93**, 040502 (2004).

[13] G. Vidal, Phys. Rev. Lett. **98**, 070201 (2007).

[14] Y.-Y. Shi *et al.*, Phys. Rev. A **74**, 022320 (2006).

[15] J. Zakrzewski *et al.*, cond-mat/0701739.

[16] P. Donohue *et al.*, Phys. Rev. B **63**, 180508(R) (2001).